




Thermal Runaway and Fire Behaviors of Lithium Iron Phosphate Battery Induced by Overheating and Overcharging

Pengjie Liu, State Key Laboratory of Fire Science, University of Science and Technology of China, Hefei 230026, China;

Shi Li, State Key Laboratory of Fire Science, University of Science and Technology of China, Hefei 230026, China; and Zhengzhou Slanpower Technology Co., Ltd., Zhengzhou 450000, China

Kaiqiang Jin, State Key Laboratory of Fire Science, University of Science and Technology of China, Hefei 230026, China;*

Weidong Fu, Zhengzhou Slanpower Technology Co., Ltd., Zhengzhou 450000, China

Chengdong Wang, Zhuangzhuang Jia, Lihua Jiang and Qingsong Wang , State Key Laboratory of Fire Science, University of Science and Technology of China, Hefei 230026, China;*

Received: 4 December 2021/**Accepted:** 21 June 2022/**Published online:** 1 August 2022

Abstract. Lithium ion batteries (LIBs) have become the dominate power sources for various electronic devices. However, thermal runaway (TR) and fire behaviors in LIBs are significant issues during usage, and the fire risks are increasing owing to the widespread application of large-scale LIBs. In order to investigate the TR and its consequences, two kinds of TR tests were conducted triggered by overheating and overcharging ways. The cells are 228 Ah with LiFePO_4 as cathode. The TR and fire behaviors were studied comprehensively from the aspect of experimental photographs, temperature characteristics, heat release rate (HRR), total heat release (THR), voltage and mass loss variation. The effects of different triggers were investigated. Under the two trigger conditions, the LIBs did not self-ignite and instead only release a large amount of gases or aerosols. With external ignition sources, the combustion process can be classified into four stages. The relationship between TR and fire behaviors related to the two conditions are discussed, respectively. Compared with overheating, the batteries burn more violently and have higher fire risks during overcharging tests. The work is supposed to provide valuable fundamental data and theory guidance for early warning technology and fire protection.

Keywords: Lithium ion battery safety, LiFePO_4 cell, Fire behaviors, Thermal runaway, Overheating, Overcharging

*Correspondence should be addressed to: Kaiqiang Jin, E-mail: jinkq@ustc.edu.cn; Qingsong Wang, E-mail: pinew@ustc.edu.cn



1. Introduction

State-of-the-art lithium ion batteries (LIBs), with high specific energy density and excellent cycle-life, are becoming the preferred storage solutions. With a range of formats, designs and cathode materials, LIBs are configurable and versatile for various application fields, ranging from portable electronics to electric vehicles (EVs) and grids storage [1, 2]. Despite their widespread popularity, there are many significant safety issues related to violent thermal runaway (TR) events [3]. Such safety concerns are heightened in automotive and aeronautic, where the failures can endanger consumer lives.

When working outside the stability domain, TR event, a failure mode, occurs inside LIBs and results in an uncontrollable rapid self-accelerating process with associated events, such as jet fire, unignited jet flow and even explosion [4, 5]. There are two primary categories of trigger that can lead to TR: electrical abuse and environmental failure [6]. The environmental failure is commonly including temperature cycling, pressure impact (altitude) and thermal abuse as well as mechanical abuse. Subsequently, a series of major exothermic reactions reported during TR are as follows: solid electrolyte interphase (SEI) decomposition, internal short circuit (ISC), the redox reaction between electrodes and electrolyte as well as the cathode and anode reactions [7]. These reactions involving in battery components can be identified with thermal analysis tools to elucidate the thermal behaviors, such as the onset temperature and heat release [8, 9].

There have been some researches concerning fire behaviors of LIBs induced by overheating, which mainly investigated the effect of various factors on LIB's fire features, such as state of charge (SOC) [10–13], cathode materials [14–17], environment pressure [18–21] and state of health (SOH) [22, 23]. Mao et al. [13] conducted fire tests on 18,650-type LIBs, and proposed that the fire risks increased with the ascending SOC. Yuan et al. [17] performed TR tests on 18,650-type LIBs with different cathodes and found that the fire risks depended significantly on cathode compositions. Chen et al. [18] studied the fire behaviors of LIBs under different environmental pressures, and revealed that the lower pressure can weaken the fire intensity. All these investigations mentioned above are focused on small capacity LIBs. Increased capacity causes the increasing fire hazards owing to more energetic substances stored. Liu et al. [24] systematically investigated the fire behaviors of 243Ah LiFePO₄ (LFP)/graphite LIBs with different SOC's induced by overheating, and analyzed the mechanism of jet fire. Wang et al. [25] studied the combustion features of 50 Ah LiNi_xCo_yMn_{1-x-y}O₂(NCM)/graphite batteries with different heating methods and concluded that the electric furnace possessed higher fire risks than the cylindrical heater. Peng et al. [26] experimentally investigated the gas toxicity and thermal hazard of 68 Ah LiFePO₄/graphite LIBs and found that the toxic and thermal hazards increased with the SOC.

Various investigations have also been carried out to study the TR behaviors induced by overcharging. The two primary features are heat and gas generation throughout the overcharging process owing to the side reactions and ohmic internal resistance. Tobishima et al. [27] performed the overcharging tests with differ-

ent charging currents at ambient temperature, and concluded that the amount of heat and gas generation increased with the charging current. Ye et al. [28] investigated the influence of charging regime on overcharging behaviors under adiabatic condition and found that the LIBs overcharged with galvanostatic-potentiostatic-galvanostatic charging regime are more dangerous. Ouyang et al. [29] compared the overcharging and over-discharging behaviors of 18,650-type LIBs and revealed that overcharging failure is more dangerous. As for the large capacity LIBs, Jiang et al. [30] performed overcharging tests on 43 Ah $\text{LiNi}_{0.5}\text{Co}_{0.2}\text{Mn}_{0.3}\text{O}_2/\text{C}$ LIBs with different charge rates and proposed that the fire hazards of battery increased with the charge rates. Huang et al. [31] investigated the TR characteristics of 40 Ah NCM pouch and prismatic LIBs in the overcharging experiments, and concluded that the prismatic battery had better TR buffering characteristic and smaller deformation owing to the safety valve. Sun et al. [32] compared the TR behaviors of battery module with LiFePO_4 under different overcharging conditions, and found that no TR occurred after stopping the overcharging with safety valve opening.

The use of large-scale LIBs is increasing with development of EVs and energy storage systems (ESS) under the growing demand for large capacity. Additionally, the large-scale batteries can reduce the pack complexity and the number of LIBs required. The fire of large-scale LIBs is more violent and spread more quickly. In consideration of the above needs, it is necessary to investigate the TR and fire behaviors of large capacity cells. The aforementioned researches covered the overheating behaviors of large-scale LFP cells. However, few studies have been conducted on overcharging tests of LFP cells with capacity of over 100 Ah. The goal of our work is to fill the knowledge gap.

During the storage and practical application, the batteries are sometimes exposed to the overheating and overcharging risks owing to malfunction of charge control and inappropriate battery management. To the best of our knowledge, the detailed comparison of fire behaviors of different triggers tested on large capacity LFP cells is missing in the current work. The quantitative analysis of the TR behaviors is also needed as such the information is significant for both fire simulation and fire risk analysis. Thus, in this study, the overheating and overcharging tests were performed to compare the TR characteristics of large capacity LFP cells under different triggers. The heat accumulation and heating power of different triggers were calculated quantitatively.

In this work, the 228 Ah $\text{LiFePO}_4/\text{graphite}$ cells, one of the most promising LIBs for electric buses and energy storage system, were employed to investigate the TR characteristics and fire behaviors in overheating and overcharging tests. A series of combustion dynamical parameters were recorded and analyzed, including experimental photographs, temperature characteristics, HRR, voltage and mass loss variation. The effects of different triggers were investigated. The relationship between TR and fire behaviors was also discussed.

2. Experimental

2.1. Battery Samples

The investigated prismatic cells are fresh large-scale power LIBs designed for electric buses or energy storage system. The battery samples employ LiFePO₄/graphite as electrodes with the nominal capacity of 228 Ah. The physical dimension is 170 mm in length, 200 mm in height and 53 mm in height width. The 228Ah LIBs contain two jelly-rolls connected in parallel. The characteristics of the battery samples are concluded in Table 1. During the sample preparation, all batteries were evaluated using constant-current (CC) and constant-voltage (CV) methods, and then prepared to 100% SOC before the fire tests.

The experiments consist of two parts: Case 1. Overheating tests, i.e. the TR was triggered by overheating. Case 2. the TR was triggered by overcharging. The battery samples, initial SOC and test setup of these two cases are the same.

2.2. Experimental Apparatus

Figure 1 shows the schematic diagram of experimental platform. The apparatus is fabricated following ISO5660 and ISO9705 and contains two main subsystems. The left part of the test rig is a combustion chamber (1.8 m × 1.8 m × 2 m) and set the sample under well controlled conditions. The right part is the analysis and exhaust system to obtain temperature, HRR, voltage and mass loss variation.

The smoke gases were collected entirely through an exhaust hood and transferred to a 300 mm diameter sampling duct. The flow rate and temperature of the smoke gases were measured by a pitot tube and thermocouples, respectively. After the steady flow zone, the gas mixture was filtrated, dried and then conveyed to the Servpro gas analyzer to help determine the HRR based on the oxygen exhaust principle [33]. A digital video was utilized to capture the combustion behaviors. The battery was laid on an electric balance to simultaneously monitor the mass variation during combustion process. In the preliminary tests, the LIBs did not self-ignite, and instead only release a large amount of gases and aerosols. In such conditions, a multi-purpose gas lighter was utilized to ignite the flammable substances.

Table 1
Basic Parameters of the LIB Samples

Parameter	Value
Geometry (length × thickness × height)/mm ³	170 × 30 × 200
Nominal capacity /Ah	228
Working voltage /V	2.5 ~ 3.6
Cathode	LiFePO ₄
Anode	Graphite
Mass/g	4130

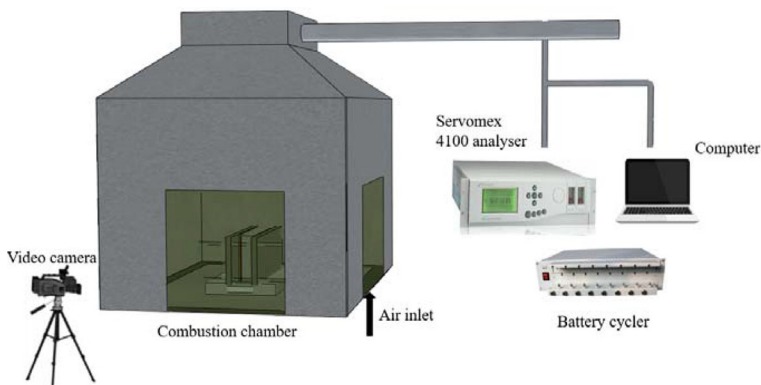


Figure 1. Schematic diagram of the burning test apparatus.

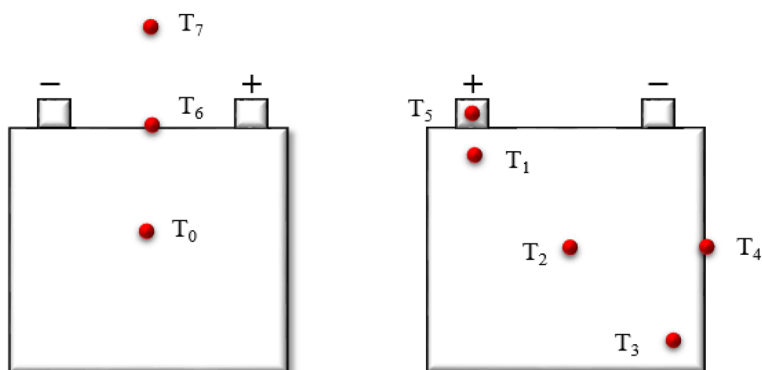


Figure 2. The arrangement of the thermocouples during the experiments.

A schematic diagram of the thermocouple setup is illustrated in Fig. 2. In overheating and overcharging tests, five K-type thermocouples (1 mm) were arranged on the battery surface to measure temperature variations during fire tests. They were pasted on the cathode tab, safety valve and the surface of the cell, respectively. The remaining 1 thermocouple, numbered as TC7, was located at 10 cm away from the safety valve to record the flame temperature.

2.2.1. Overheating Tests In this section, homogeneously external heating of the largest surfaces of LIBs was performed to obtain the TR characteristics triggered by overheating. Figure 3a presents a schematic diagram of the overheating test setup. An electric heating plate (200 mm length, 170 mm width) was utilized as the external heating source against the battery surface. The output power of the heating plate was 500 W. A 5 mm thick ceramic fiber blanket was placed uniformly around the battery and heater to prevent excessive heat dissipation. A tailored sample holder, consisting of two stainless steel plates, was employed to fix the bat-

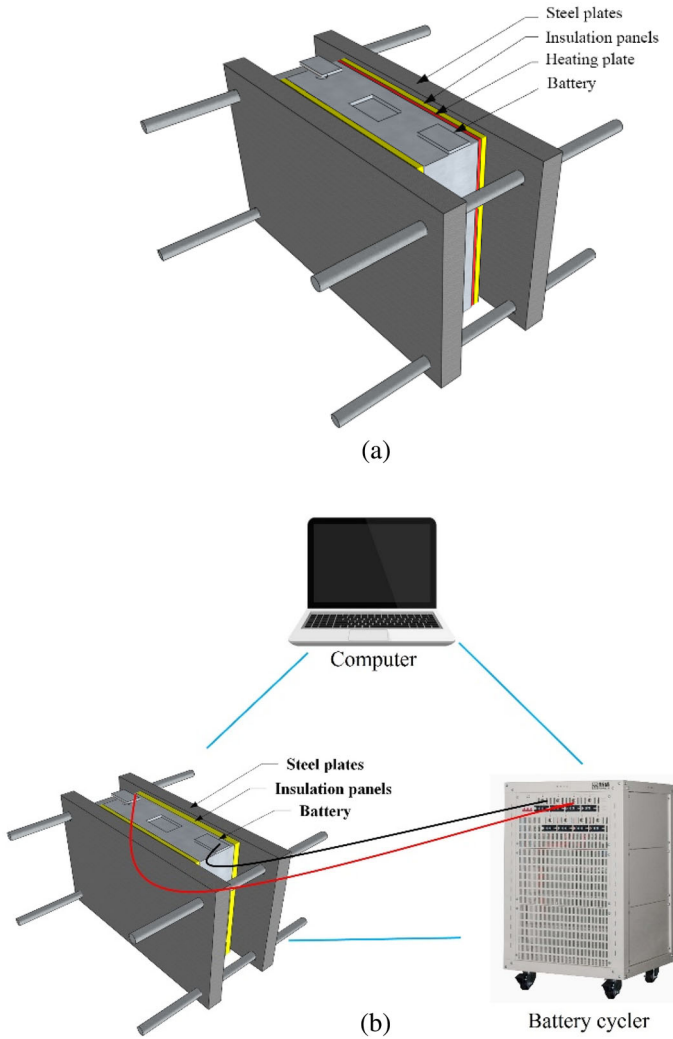


Figure 3. The schematic diagram of the experimental setup. (a) Overheating tests and (b) overcharging tests.

tery to ensure a good thermal contact between the heater and battery. The heating plate was turned off when the LIBs fire burnt out. The selected SOC was 100%. A battery cycler was used to record the battery's voltage variation.

2.2.2. Overcharging Tests In this part, the overcharging tests were conducted in the combustion chamber. Figure 3b shows the related experiment set up. First, before overcharge tests, the cells were pre-cycled and charged to 100% SOC. Then the overcharging tests with 0.2C was performed without any protection sets at a

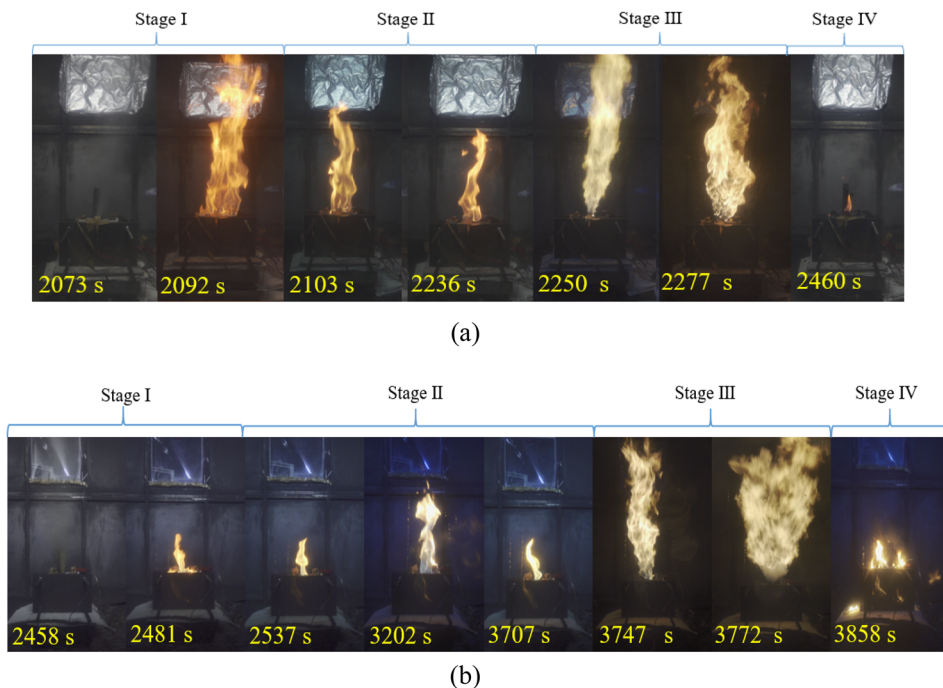


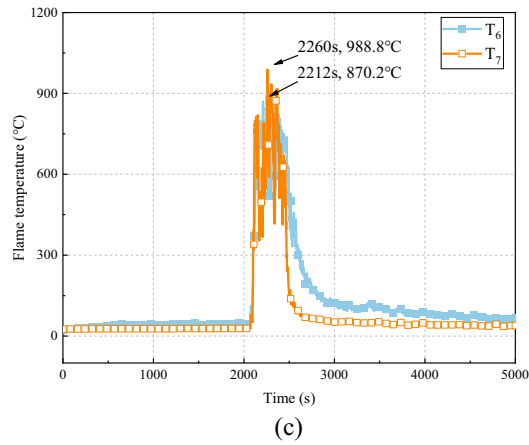
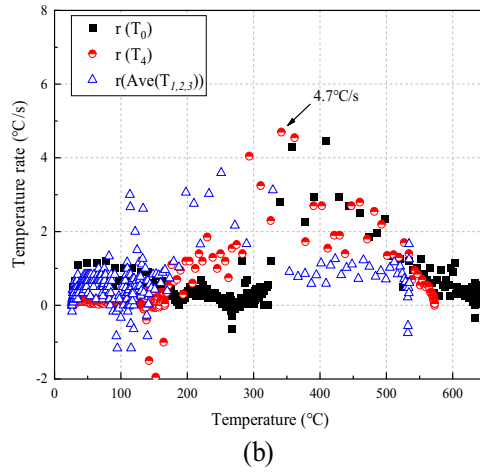
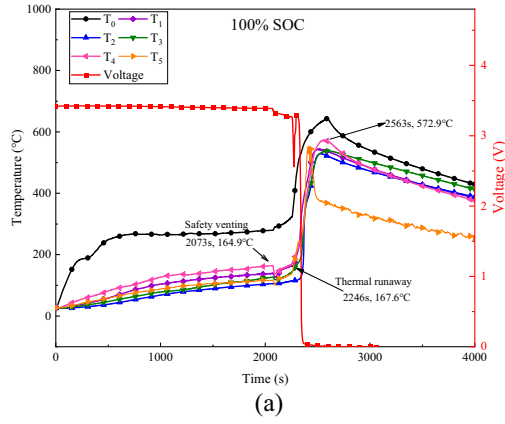
Figure 4. The fire behaviors of LIBs under different TR triggers. (a) Overheating tests and (b) overcharging tests.

constant current charge protocol. Charge the cell from 100% SOC until the TR occurs, representing the scenario of the continuous overcharge after charging. The voltage and current variation were recorded by a power supply (Neware BTS 30 V/50 A). The final SOC was determined by coulomb counting (integrate current (A) over time). The sample holder and ceramic fiber blanket were also utilized to ensure that the battery was stable and less heat was dissipated, respectively.

3. Results and Discussion

3.1. Combustion Behaviors

Figure 4a and b describe the representative combustion phenomenon corresponding to various timestamps in the overheating and overcharging triggered TR tests, respectively. For the LIBs with different triggering modes, the overall combustion process gave the similar trends. According to the manifestation of burning behavior and the mass loss curve, the combustion process can be divided into several stages: (I) safety venting and ignition, (II) stable combustion, (III) thermal runaway and jet flame as well as (IV) abatement and extinguishment.



◀Figure 5. The temperature variations of LIBs in overheating tests. (a) The surface temperature, (b) The temperature rate as well as (c) The flame temperature.

During the whole test process, the LIBs were constant heated and charged by the electric heater and battery cycler, respectively. During this stage, multiple physical and chemical reactions occur inside the LIBs, depending on the abuse scenario. The physical reactions are the evaporation of electrolytes, and the chemical transformations are mainly the side reactions to generate flammable hydrocarbons [34, 35]. The two above increases the pressure in the cell. After continuous heating and charging, the inner pressure increased and the safety valve opened at 2073s and 2458s for overheating and overcharging tests, respectively, accompanied by a loud crack sound.

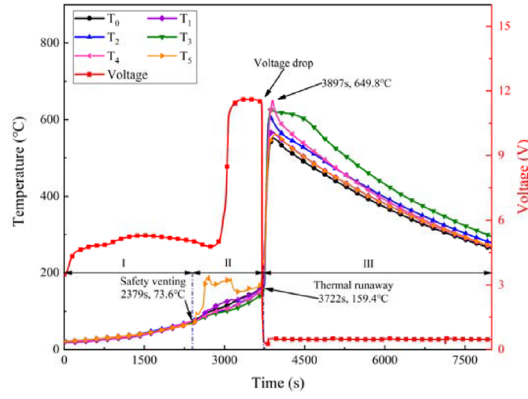
For overheating tests, the main form of electrolyte inside cell is liquid owing to the limitation of the saturated vapor pressure. With the safety valve opening, the internal pressure relieves abruptly from the saturation pressure to ambient pressure, which accelerates the electrolyte boiling. Thus, a short continuous venting event was observed and accumulated in combustion chamber, which formed a deflagration fireball after ignition. Unlike overheating tests, no continuous venting occurred for overcharging tests because the gaseous products have dominant contribution to pressure. And only the electrolyte liquid was observed at the instant of the safety valve opening.

Afterward, the batteries entered the stable combustion stage and this phenomenon lasted 148 s and 1256 s for LIBs under overheating and overcharging modes, respectively. During stage II, the flame became stable and small under the evaporation of organic solvent and gas generation. Hereafter, an aggressive cylindrical jet flame occurred in the vertical direction. After the TR burst, for overheating tests, there are multiple characteristics fire behaviors, such as jet fire weakening and jet fire increasing again, while as for overcharging tests, the jet flame intensity became more severe than the former, which are described in detail in Sect. 3.6. The TR stage lasted for 143 s and 96 s under overheating and overcharging tests, respectively. Subsequently, the LIBs fire decayed until extinguishment.

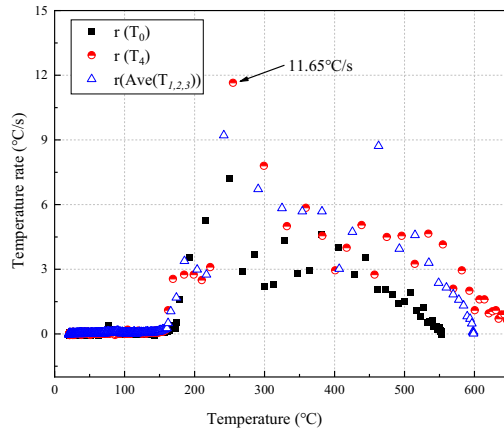
3.2. Temperature Variations

3.2.1. Overheating Tests The temperature is a significant parameter to characterize the reaction process and thermal hazards. As shown in Fig. 5a, the temperatures at different locations did not follow the same increase trend. T_0 increased quickly, while the other temperatures increased almost linearly due to thermal conduction through the jelly roll from the heating plate.

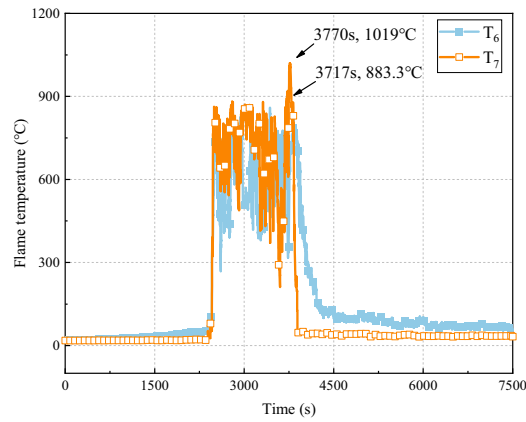
After continuous heating, the battery temperature gradually increased and the self-heating reactions were triggered. At 2073s, when T_4 was 164.9°C and T_2 was 105.9°C, the safety valve opened, which was larger than the boiling points of electrolyte. Note that there is a sharp drop of battery temperature owing to the vent-



(a)



(b)



(c)

◀ **Figure 6. The temperature variations of LIBs in overcharging tests. (a) The surface temperature, (b) The temperature rate as well as (c) The flame temperature.**

Table 2
The Summary of Average Heating Power (P_{h-ave}) at Different Stages

Abuse type	P_{h-ave} (W) Stage I	P_{h-ave} (W) Stage II	P_{h-ave} (W) Stage III
Overheat	360.49	526.2	4296.25
Overcharge	96.58	254.48	7574.75

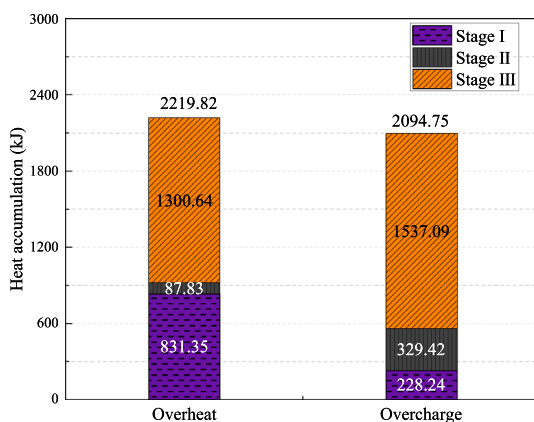
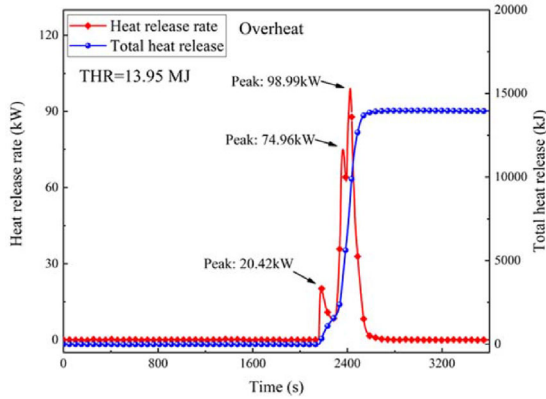


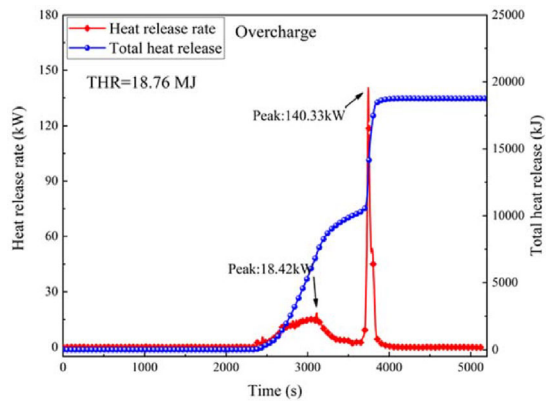
Figure 7. Heat accumulation in overheating and overcharging tests.

ing of high-temperature ejecta and electrolyte. The values of temperature drop (T_d) vary with the thermocouples' positions. The biggest T_d occurs on the side surface and the value is 27.6°C. The onset temperature of TR is the critical point where a steep increase in temperature rate starts. The TR occurred at onset temperature of 170.2°C for T_4 and the increasingly exothermic reactions were triggered. Specifically, the maximum surface temperature and temperature rate were 572.9°C and 4.7°C/s, respectively. The highest observed flame temperature was 988.8°C at 10 cm above safety valve.

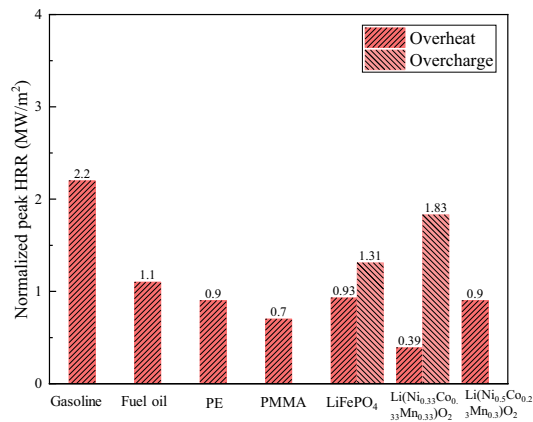
3.2.2. *Overcharging Tests* Figure 6 shows the surface and flame temperature variations of LIBs during overcharging process. As exhibited in Fig. 6a, the temperature at different surfaces showed the same pace of increase, which was due to heat generated from the side reactions inside the battery. Two venting events can also be observed in the overcharging trigger: a minor venting at safety venting due to



(a)



(b)



(c)

◀Figure 8. The HRR curves and THR for LIBs under different triggers. (a) Overheating, (b) Overcharging as well as (c) The normalized peak HRR in comparison with that of the standard combustible substances [12] and other battery [10, 38].

the gas products accumulated, and a major venting accompanied by vigor venting gaseous mixture and particle during TR.

In the first stage, the combination of over-voltage heat, reversible and side reaction heat increased the battery temperature continuously. At 2379 s, when T_4 was 73.6°C and T_2 was 73.4°C, the first venting (safety venting) occurred and the additional overcharging capacity was 33.66 Ah. The temperature of safety venting is smaller than the boiling points of electrolyte, which means that the gaseous products have dominant contribution to pressure rather than electrolyte vapor. Note that no measurable temperature drop occurred at safety venting, which because it was mainly caused by the phase change of electrolyte absorbing large amounts of heat. When the additional overcharging capacity exceeded 44.14 Ah, the LIBs entered TR stage and the violent jet flame was observed. Specifically, the peak surface temperature and temperature rate were 649.8°C and 11.65°C/s, respectively. The maximum temperature rate is 2.5 times higher than that of overheating tests. The peak flame temperature was 1011.2°C at 10 cm above safety valve.

3.2.3. Comparison of TR Characteristics Induced by Overheating and Overcharging The heat accumulation and heating power are two critical parameters to characterize the TR propagation and mitigation. To better compare the TR hazards induced by overheating and overcharging, the heat accumulation (HA) and heating power (P_h) were introduced to quantify thermal hazards. The P_h can be roughly calculated with Eq. (1).

$$P_h = c_b m_b \frac{dT_{ave}}{dt} \quad (1)$$

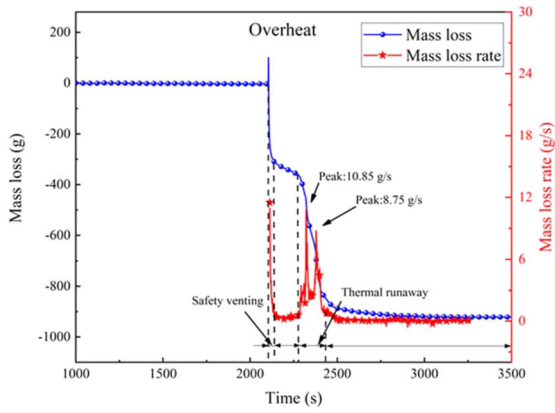
where T_{ave} is the average surface temperature of the battery, $c_b = 1.1 \text{ kJ kg}^{-1} \text{ } ^\circ\text{C}^{-1}$ is the LIB specific heat capacity. m_b is the battery mass and can be measured by the electrical balance.

For overcharging tests, since the temperature difference between the battery surfaces is very small, thus the HA during overcharging can be expressed with Eq. (2). Where T_0 is the initial temperature of the battery.

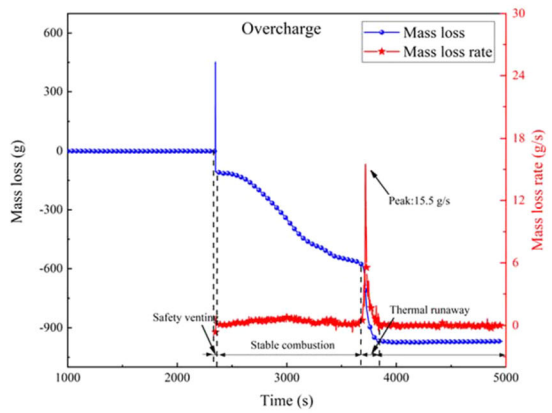
$$HA = c_b m_b (T_{ave} - T_0) \quad (2)$$

While for overheating tests, there is a huge temperature gradient of LIBs in the thickness direction before TR. The HA before TR can be computed as follows:

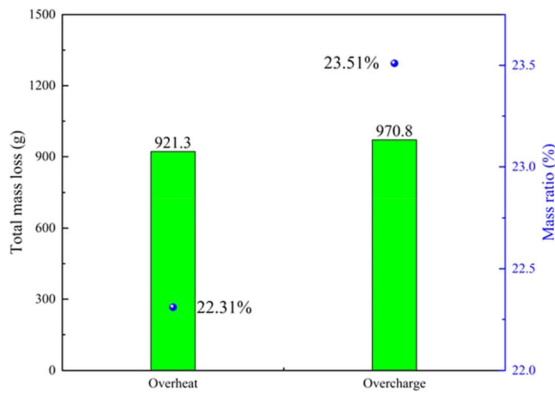
$$HA = \int \rho_b A_b c_b (T_b(x) - T_0) dx \quad (3)$$



(a)



(b)



(c)

◀Figure 9. The mass loss and mass loss rate for LIBs under different triggers. (a) Overheating, (b) Overcharging as well as (c) The total mass loss.

Furthermore, The HA during TR can be roughly determined by Eq. (4). $m_{b,tr}$ represents the battery mass after the TR tests.

$$HA = c_b m_{b,tr} (T_{max} - T_{tr}) \quad (4)$$

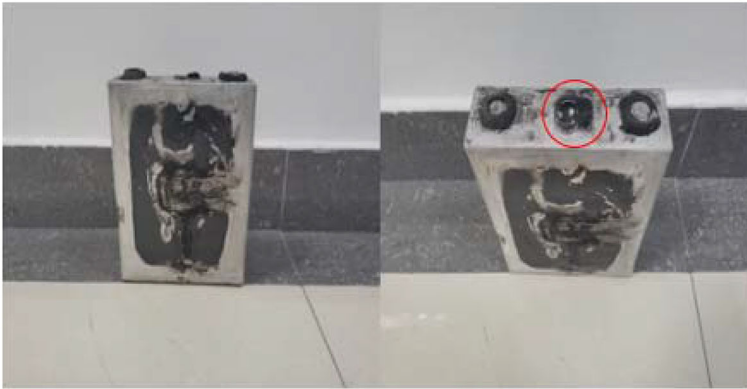
The average heating power (P_{h-ave}) was introduced to characterize the heating power of the battery at different stages. The calculation results have been reported in Table 2. Compared with the P_{h-ave} at stage I, note that the value of P_{h-ave} under overheating is 3.73 times larger than that of overcharging due to the heating plate. During stage II, the P_{h-ave} increases significantly owing to the increasing side reactions. While as for stage III, the P_{h-ave} reaches its peak and the P_{h-ave} under overcharging is larger owing to more electric energy stored. Figure 7 presents the HA under overheating and overcharging. The characteristics of HA in different stages under overcharging are different from that of overheating. The HA are 2219.82 kJ and 2094.75 kJ for overheating and overcharging tests, respectively. Compared with overheating tests, the stage II and stage III possess higher risks from the perspective of thermal hazards.

3.3. Heat Release Rate

The HRR is one of the most critical variables to characterize the fire intensity and fire hazards quantitatively. The HRR is the energy release rate of flaming combustion and a numerical integration of HRR can determine the total heat release (THR).

Figure 8 present the HRR curves versus time of the LIBs in overheating and overcharging tests, respectively. The change of HRR with time corresponds to the combustion behaviors of LIBs. As illustrated in Fig. 8a, for the overheating tests, the three peaks pertain to two segments associated with those two venting events. For overheating tests, the first peak HRR occurred at safety venting and was arising from the gas accumulated before burning. The first peak HRR was 20.42 kW and the value was influenced by the ignition moment. Two subsequent HRR peaks are corresponding to the fast-exothermic reactions (TR) process of the two jelly-rolls. The two peak HRR values were 74.96 kW and 98.99 kW, respectively.

While as for the overcharging tests, only one peak HRR was observed during the TR stage. No continuous venting occurred at safety valve opening for overcharging tests due to the lower venting temperature, thus the first peak HRR was not observed. And only one peak HRR occurred during TR stage, which means that the TR process interval between the two jelly-rolls was very short or occurred simultaneously. By dividing HRR with the total surface area of the battery, the normalized peak HRR is compared with standard combustible substances, as shown in Fig. 8c. The resulting values in overheating and overcharging tests are



(a)



(b)

Figure 10. The combustion residues of LIBs under different triggers. (a) Overheating, (b) Overcharging.

0.93 and 1.31 MW/m², and slightly higher than that of PE and fuel oil, respectively. The calculated THR values are 13.95 and 18.76 MJ for overheating and overcharging tests, respectively. For comparison, the normalized peak HRR of fully charged LIBs with different cathodes are presented in Fig. 8c. These results from the limited comparison indicate that the HRR is highly dependent on the cathode composition and the increase of Ni vastly intensify the fire severity of LIBs. For different chemistries, the batteries burn more violently and possess higher fire risks during overcharging.

3.4. Mass Loss and Residue

Figure 9 presents the mass loss curves during overheating and overcharging tests. By subtracting the initial mass of the battery, the masses are normalized, thus the mass losses are negative values. Note that the mass loss variations show the simi-

lar trend during overheating and overcharging tests and are summarized into four stages, which are ascribed to the complex and varied internal reactions.

At the first stage, the batteries were well sealed, thus the mass fluctuated slightly, and a little smoke was observed owing to the decomposition and melting of the plastic packaging of LIBs. At the instant of safety valve opening, the violent and sudden ejection exerted a reactive force on the balance and was shown as the rebound in mass-loss value. Afterward, the LIBs entered the transition stage. During this stage, the mass loss changed gently owing to the less gas generation and the evaporation of electrolyte. The mass loss rates were about 0.37 g/s and 0.36 g/s at the transition phase in overheating and overcharging tests, respectively. Hereafter, a sharp mass decrease was observed during TR phase with the vigorous ejection. During this process, there are two mass loss rate peaks in overheating tests and one mass loss rate peak in overcharging tests, respectively, which are corresponding to the HRR peaks. Note that the mass loss at TR stage accounts for most of the mass loss. In the final stage, the mass showed a slight decrease until the reactants were depleted and no substances ejected out from the safety valve.

The mass loss ratio can be obtained by dividing the total mass loss with the initial mass of the battery. Figure 9c shows the total mass loss and mass loss ratio in overheating and overcharging tests, respectively. The values of peak mass loss rate are 10.85 g/s and 15.5 g/s, and the total mass loss is 921.3 g and 970.8 g for cells in overheating and overcharging tests, respectively. These values indicate that the overcharging tests cause more substances to be ejected out and the venting process is more violent. That can be also characterized by the residues of the batteries. As exhibited in Fig. 10, more severe damage and deformation appear on the batteries after overcharging. In overheating and overcharging tests, the formation of small aluminum beads means that the maximum inner temperature exceeds the aluminum's melting point of 660.4°C.

3.5. Investigation of the Overheating and Overcharging Mechanisms

3.5.1. Overheating Tests The 228 Ah battery consists of two jelly-rolls connected in parallel. The large format LIBs were locally heated on the front surface. Thus, the TR process is firstly triggered on the jelly roll close to the heating plate, and then expands to the second jell roll. During continuous heating process, the combination of electrolyte vapor and gas increases the internal pressure inside cells. With the temperature increase, the solid electrolyte interface (SEI) layer decomposes firstly at the relatively low temperature [36]. Afterwards, the intercalated Li^+ can react with the electrolyte and release heat and gases [34, 35]. After safety venting, the solvents accelerate boiling owing to the higher temperature, then form a short continuous jet. As the temperature further increases, the separators shrink and collapse, which leads to internal short circuit. The electrical energy stored releases a large amount of Joule heat. The delithiated Li_0FePO_4 can decompose and release O_2 [37], which would react with active materials. As the above fast exothermic reactions occur, the TR process of LIBs is activated, and jet flame can be observed.

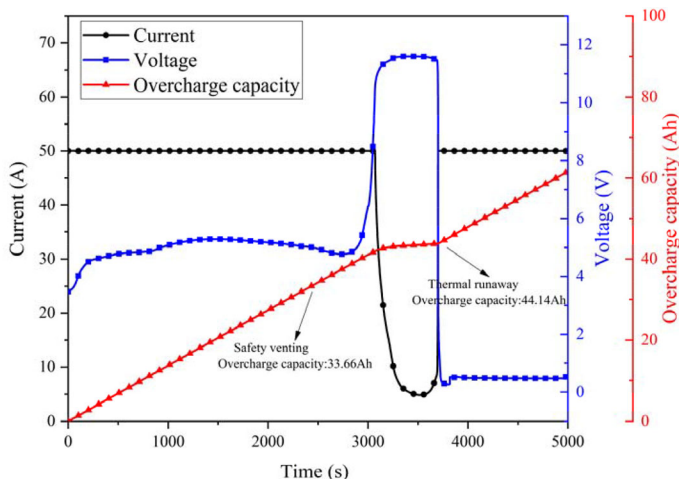


Figure 11. Voltage, current, overcharge capacity variations over time in overcharging tests.

3.5.2. Overcharging Tests In order to further evaluate the overcharging behaviors and mechanisms, the variations of overcharging capacity, voltage and current over time are presented in Fig. 11. According to the two characteristic events, i.e., safety venting and TR, the overcharging process can be simply classified as three stages. At the initial stage of overcharging tests, the voltage increases because the Li^+ deintercalated from the cathode and intercalates anode. When the batteries are overcharged into 4.5 V, the voltage rises slowly. After continuous overcharging, the deintercalation and intercalation rates in cathode and anode slow down during this process. With the voltage increase, the reactions of the lithium dendrites in anode with electrolyte, the oxidative decomposition of electrolyte and the collapse of cathode can occur and generate large amounts of gases to increase the internal pressure. These reactions also cause the voltage to drop slowly. Hereafter, a rapid increase in voltage can be observed at 2808 s owing to the further increase of Li^+ intercalation into the anode, the decrease of electrolyte and the change of distance between electrodes by gas generation, which increase the degree of internal polarization. When the overcharging capacity reaches 43.11 Ah, there is an apparent voltage platform area (around 11.6 V), and is the balance of the overcharging process and the internal micro short circuit [30]. The internal short circuit is caused by the formation of the lithium dendrites piercing the separator. After the overcharging capacity exceeding 44.14 Ah, the voltage drops and the separator melts. The voltage drop area is a stage where thermal runaway occurs, side reactions and internal short circuit occur violently [28]. These reactions release large amounts of heat and increase the battery temperature rapidly.

4. Conclusions

In this work, the 228 Ah LiFePO₄/graphite cells, one of the most promising LIBs for electric buses and energy storage, were employed to investigate the TR characteristics and fire behaviors in overheating and overcharging tests. A series of combustion dynamical parameters were recorded and analyzed, including experimental photographs, temperature characteristics, HRR, voltage and mass loss variation. The effects of different triggers were investigated. The relationship between TR and fire behaviors was also discussed. Furthermore, the TR characteristics triggered by overcharging and overheating are comparatively analyzed. The main conclusions are summarized as following:

In overheating and overcharging tests, the LIBs did not self-ignite and instead only release a large amount of gases or aerosol droplets. With external ignition sources, the combustion process can be divided into the following stages: safety venting and ignition, stable combustion, thermal runaway and jet flame, abatement and extinguishment.

Compared with overcharging tests, a short continuous venting event was observed at safety valve opening, and the cooling effect of the safety valve opening is more obvious during overheating process. A large temperature gradient within the cell occurred during overheating process, while the LIB temperature distribution is homogeneous in overcharging tests. In overcharging tests, the stage II and stage III possess higher risks from the perspective of thermal hazards. The maximum temperature rate reaches 11.65°C/s and is 2.5 times higher than that of overheating tests. The maximum surface temperatures are 572.9°C and 649.8°C for overheating and overcharging tests, respectively. Compared with overheating, the batteries burn more violently and have higher fire risks during overcharging, which induce more mass loss and heat release of flaming combustion. The peak HRR can be as high as 98.99 kW and 140.33 kW for overheating and overcharging tests, respectively.

The observations presented in this work provide an insight of the burning behaviors and TR characteristics under overheating and overcharging triggers. A comprehensive analysis of TR process and fire risks is significant. Such results can serve as scientific references for safety applications and fire protection.

Acknowledgements

This work is supported by the National Key R&D Program of China (No. 2021YFB2402001), the Key Research and Development Plan of Anhui Province (No. 202104a07020003), the project funded by China Postdoctoral Science Foundation (No. 2022T150615), and the Fundamental Research Funds for the Central Universities (No. WK2320000051). Dr. Q.S Wang is supported by Youth Innovation Promotion Association CAS (No.Y201768).

References

1. Wang F, Harindintwali JD, Yuan ZZ, Wang M, Wang FM, Li S et al (2021) Technologies and perspectives for achieving carbon neutrality. *Innovation*. 2(4):100180. <https://doi.org/10.1016/j.xinn.2021.100180>
2. Wang QS, Mao BB, Stolarov SI, Sun JH (2019) A review of lithium ion battery failure mechanisms and fire prevention strategies. *Progress Energy Combustion Sci*. 73:95–131. <https://doi.org/10.1016/j.pecs.2019.03.002>
3. Feng XN, Ren DS, He XM, Ouyang MG (2020) Mitigating thermal runaway of lithium-ion batteries. *Joule*. 4(4):743–70. <https://doi.org/10.1016/j.joule.2020.02.010>
4. Liu P, Liu C, Yang K, Zhang M, Gao F, Mao B et al (2020) Thermal runaway and fire behaviors of lithium iron phosphate battery induced by over heating. *J Energy Storage*. 31:101714. <https://doi.org/10.1016/j.est.2020.101714>
5. Liu P, Sun H, Qiao Y, Sun S, Wang C, Jin K et al (2022) Experimental study on the thermal runaway and fire behavior of LiNi_{0.8}Co_{0.1}Mn_{0.1}O₂ battery in open and confined spaces. *Process Safety Environ Protect*. 158:711–26. <https://doi.org/10.1016/j.psep.2021.12.056>
6. Wang QS, Ping P, Zhao XJ, Chu GQ, Sun JH, Chen CH (2012) Thermal runaway caused fire and explosion of lithium ion battery. *J Power Sources*. 208:210–24. <https://doi.org/10.1016/j.jpowsour.2012.02.038>
7. Xuning F, Minggao O, Xiang L, Languang L, Yong X, Xiangming H (2018) Thermal runaway mechanism of lithium ion battery for electric vehicles: a review. *Energy Storage Mater (Netherlands)*. 10:246–67. <https://doi.org/10.1016/j.ensm.2017.05.013>
8. Kvasha A, Gutierrez C, Osa U, de Meatza I, Blazquez JA, Macicior H et al (2018) A comparative study of thermal runaway of commercial lithium ion cells. *Energy*. 159:547–57. <https://doi.org/10.1016/j.energy.2018.06.173>
9. Wang QS, Sun JH, Yao XL, Chen CH (2005) Thermal stability of LiPF₆/EC+DEC electrolyte with charged electrodes for lithium ion batteries. *Thermochimica Acta*. 437(1–2):12–6. <https://doi.org/10.1016/j.tca.2005.06.010>
10. Zhong GB, Mao BB, Wang C, Jiang L, Xu KQ, Sun JH et al (2019) Thermal runaway and fire behavior investigation of lithium ion batteries using modified cone calorimeter. *J Thermal Anal Calorim*. 135(5):2879–89. <https://doi.org/10.1007/s10973-018-7599-7>
11. Said AO, Lee C, Liu X, Wu Z, Stolarov SI (2019) Simultaneous measurement of multiple thermal hazards associated with a failure of prismatic lithium ion battery. *Proc Combust Inst*. 37(3):4173–80. <https://doi.org/10.1016/j.proci.2018.05.066>
12. Ribiere P, Grugeon S, Morcrette M, Boyanov S, Laruelle S, Marlair G (2012) Investigation on the fire-induced hazards of Li-ion battery cells by fire calorimetry. *Energy Environ Sci*. 5(1):5271–80. <https://doi.org/10.1039/c1ee02218k>
13. Mao B, Chen H, Jiang L, Zhao C, Sun J, Wang Q (2020) Refined study on lithium ion battery combustion in open space and a combustion chamber. *Process Safety Environ Protect*. 139:133–46. <https://doi.org/10.1016/j.psep.2020.03.037>
14. Chen MY, Ouyang DX, Weng JW, Liu JH, Wang J (2019) Environmental pressure effects on thermal runaway and fire behaviors of lithium-ion battery with different cathodes and state of charge. *Process Safety Environ Protect*. 130:250–6. <https://doi.org/10.1016/j.psep.2019.08.023>
15. Liu X, Wu ZB, Stolarov SI, Denlinger M, Masias A, Snyder K (2016) Heat release during thermally-induced failure of a lithium ion battery: Impact of cathode composition. *Fire Safety J*. 85:10–22. <https://doi.org/10.1016/j.firesaf.2016.08.001>

16. Said AO, Lee C, Stolarov SI (2020) Experimental investigation of cascading failure in 18650 lithium ion cell arrays: impact of cathode chemistry. *J Power Sources*. 446:227347. <https://doi.org/10.1016/j.jpowsour.2019.227347>
17. Yuan L, Dubaniewicz T, Zlochower I, Thomas R, Rayyan N (2020) Experimental study on thermal runaway and vented gases of lithium-ion cells. *Process Safety Environ Protect*. 144:186–92. <https://doi.org/10.1016/j.psep.2020.07.028>
18. Chen M, Liu J, He Y, Yuen RKK, Wang J (2017) Study of the fire hazards of lithium-ion batteries at different pressures. *Appl Thermal Eng*. 125:1061–74
19. Fu YY, Lu S, Shi L, Cheng XD, Zhang HP (2018) Ignition and combustion characteristics of lithium ion batteries under low atmospheric pressure. *Energy*. 161:38–45. <https://doi.org/10.1016/j.energy.2018.06.129>
20. Liu Q, Yi X, Han X (2020) Effect of different arrangement on thermal runaway characteristics of 18650 lithium ion batteries under the typical pressure in civil aviation transportation. *Fire Technol*. 56(6):2509–23. <https://doi.org/10.1007/s10694-020-00984-0>
21. Wang H, Du Z, Liu L, Zhang Z, Hao J, Wang Q et al (2020) Study on the thermal runaway and its propagation of lithium-ion batteries under low pressure. *Fire Technol*. 56(6):2427–40. <https://doi.org/10.1007/s10694-020-00963-5>
22. Wang Z, Wang J (2020) An experimental investigation of the degradation and combustion behaviors associated with lithium ion batteries after different aging treatments. *J Cleaner Production*. 272:122708. <https://doi.org/10.1016/j.jclepro.2020.122708>
23. Xie S, Ren LX, Yang XY, Wang HB, Sun Q, Chen XT et al (2020) Influence of cycling aging and ambient pressure on the thermal safety features of lithium-ion battery. *J Power Sources*. 448:227425. <https://doi.org/10.1016/j.jpowsour.2019.227425>
24. Liu P, Li Y, Mao B, Chen M, Huang Z, Wang Q (2021) Experimental study on thermal runaway and fire behaviors of large format lithium iron phosphate battery. *Appl Thermal Eng*. 192:116949. <https://doi.org/10.1016/j.applthermaleng.2021.116949>
25. Wang Z, Yang H, Li Y, Wang G, Wang J (2019) Thermal runaway and fire behaviors of large-scale lithium ion batteries with different heating methods. *J Hazard Mater*. 379:120730. <https://doi.org/10.1016/j.jhazmat.2019.06.007>
26. Peng Y, Yang LZ, Ju XY, Liao BS, Ye K, Li L et al (2020) A comprehensive investigation on the thermal and toxic hazards of large format lithium-ion batteries with LiFePO₄ cathode. *J Hazard Mater*. 381:120916. <https://doi.org/10.1016/j.jhazmat.2019.120916>
27. Tobishima S-i, Yamaki J-i (1999) A consideration of lithium cell safety. *J Power Sources*. 81–82:882–6. [https://doi.org/10.1016/S0378-7753\(98\)00240-7](https://doi.org/10.1016/S0378-7753(98)00240-7)
28. Ye J, Chen H, Wang Q, Huang P, Sun J, Lo S (2016) Thermal behavior and failure mechanism of lithium ion cells during overcharge under adiabatic conditions. *Appl Energy*. 182:464–74. <https://doi.org/10.1016/j.apenergy.2016.08.124>
29. Ouyang D, Chen M, Liu J, Wei R, Weng J, Wang J (2018) Investigation of a commercial lithium-ion battery under overcharge/over-discharge failure conditions. *RSC Adv*. 8(58):33414–24. <https://doi.org/10.1039/c8ra05564e>
30. Jiang LH, Luo ZM, Wu TQ, Shao LY, Sun JH, Liu CQ et al (2019) Overcharge behavior and early warning analysis of LiNi_{0.5}Co_{0.2}Mn_{0.3}O₂/C lithium-ion battery with high capacity. *J Electrochem Soc*. 166(6):A1055–A1062. <https://doi.org/10.1149/2.0661906jes>
31. Huang L, Zhang Z, Wang Z, Zhang L, Zhu X, Dorrell DD (2019) Thermal runaway behavior during overcharge for large-format Lithium-ion batteries with different packaging patterns. *J Energy Storage*. 25:100811. <https://doi.org/10.1016/j.est.2019.100811>
32. Sun L, Wei C, Guo D, Liu J, Zhao Z, Zheng Z et al (2020) Comparative study on thermal runaway characteristics of lithium iron phosphate battery modules under different

- overcharge conditions. *Fire Technol.* 56(4):1555–74. <https://doi.org/10.1007/s10694-019-00942-5>
33. Huggett C (1980) Estimation of rate of heat release by means of oxygen-consumption measurements. *Fire Mater.* 4(2):61–5. <https://doi.org/10.1002/fam.810040202>
 34. Gachot G, Grugeon S, Eshetu GG, Mathiron D, Ribiere P, Armand M et al (2012) Thermal behaviour of the lithiated-graphite/electrolyte interface through GC/MS analysis. *Electrochimica Acta.* 83:402–9. <https://doi.org/10.1016/j.electacta.2012.08.016>
 35. Spotnitz R, Franklin J (2003) Abuse behavior of high-power, lithium-ion cells. *J Power Sources.* 113(1):81–100. [https://doi.org/10.1016/s0378-7753\(02\)00488-3](https://doi.org/10.1016/s0378-7753(02)00488-3)
 36. Wang QS, Sun JH, Yao XL, Chen CH (2006) Thermal behavior of lithiated graphite with electrolyte in lithium-ion batteries. *Journal of the Electrochemical Society.* 153(2):A329–A33. <https://doi.org/10.1149/1.2139955>
 37. Joachin H, Kaun TD, Zaghbi K, Prakash J (2009) Electrochemical and thermal studies of carbon-coated LiFePO₄ cathode. *J Electrochem Soc.* 156(6):A401–A6. <https://doi.org/10.1149/1.3106121>
 38. Huang Z, Liu J, Zhai H, Wang Q (2021) Experimental investigation on the characteristics of thermal runaway and its propagation of large-format lithium ion batteries under overcharging and overheating conditions. *Energy.* 233:121103. <https://doi.org/10.1016/j.energy.2021.121103>

Publisher's Note Springer Nature remains neutral with regard to jurisdictional claims in published maps and institutional affiliations.